



1 **Secondary formation dominated low molecular weight amines origins**
2 **in aerosols over the marginal seas of China**

3 Xiao-Ying Yang^{1,2}, Fang Cao^{1,2}, Chang-Liu Wu^{1,2}, Yu-Xian Zhang^{1,2}, Wen-Huai
4 Song^{1,2}, Yu-Chi Lin^{1,2}, Yan-Lin Zhang^{1,2*}

5 ¹. School of Ecology and Applied Meteorology and Atmospheric Environment Center,
6 Joint Laboratory for International Cooperation on Climate and Environmental Change,
7 Ministry of Education, Nanjing University of Information Science & Technology,
8 Nanjing 210044, China.

9 ². Jiangsu Key Laboratory of Atmospheric Environment Monitoring and Pollution
10 Control, Collaborative Innovation Center on Forecast and Evaluation of
11 Meteorological Disasters (CIC-FEMD), Nanjing University of Information Science &
12 Technology, Nanjing 210044, China.

13

14 ***Correspondence:** Yan-Lin Zhang (dryanlinzhang@outlook.com)

15



16 **Abstract.** Atmospheric low molecular weight amines play important roles in new
17 particle formation, aerosol properties, and climate. However, the compositions,
18 sources, and secondary formation mechanisms of amines in offshore aerosols remain
19 unclear. Here, an integrated observation of methylamine (MA), ethylamine (EA),
20 dimethylamine (DMA), iso-propanamine (IPA), propanamine (PA), “trimethylamine +
21 diethylamine” (TMDEA), and > 100 other chemical components in total suspended
22 particles was conducted during a spring 2018 research cruise across the Yellow Sea
23 and Bohai Sea, China. Concentrations of total amines exhibited a north-to-south
24 decrease from the Bohai Sea to the South Yellow Sea, corresponding to the declined
25 influence of terrestrial air masses. Source analyses were performed by evaluating the
26 linear relationships between individual amines and specific organic molecular tracers
27 representing primary biogenic sources, higher plant waxes, marine/microbial sources,
28 biogenic secondary organic aerosols (BSOA), biomass burning, and fossil fuel
29 combustion. MA, EA, and DMA were largely influenced by terrestrial biogenic and
30 anthropogenic sources, with the majority (74.0%, 52.6%, and 65.7%, respectively)
31 formed through nitrate-associated secondary formation pathways, interacting with
32 BSOA formation. PA was mainly derived from combustion-related sources, along
33 with terrestrial and marine biogenic contributions. In contrast, the predominate amine,
34 TMDEA, was mostly generated through sulfate-associated secondary formation
35 pathways (61.8%) and contributed by marine emissions, leading to the north-to-south
36 increase in its relative contribution to aerosol amines. The findings highlight distinct
37 potential sources and formation mechanisms for different amines in offshore aerosols,
38 and underscore the importance of multiphase chemistry of amines under varying
39 ambient conditions.

40



41 **1 Introduction**

42 Amines, derivatives of ammonia (NH_3) with one or more hydrogen atoms replaced by
43 alkyl or aryl groups, represent an important class of nitrogen-containing organic
44 compounds (Shen et al., 2023; Zhu et al., 2022; Liu et al., 2023). Low molecular
45 weight amines, such as methylamine (MA), dimethylamine (DMA), trimethylamine
46 (TMA), ethylamine (EA), diethylamine (DEA), and propanamine (PA), are the most
47 common and abundant atmospheric amines, which are ubiquitous in both the gas and
48 particle phases due to high water solubility and strong alkalinity (Ge et al., 2011a, b).
49 These amines are primarily emitted in the gas phase, and mainly occur as protonated
50 cations (aminium salts) in aerosols.

51 Gaseous amines can be oxidized by atmospheric oxidants (including OH, O_3 , and NO_x)
52 (Tang et al., 2013; Nielsen et al., 2012; Murphy et al., 2007), and undergo
53 gas-to-particle conversion through direct dissolution (Liu et al., 2018), acid-base
54 reactions (Liu et al., 2023; Barsanti and Pankow, 2006), and heterogeneous reactions
55 (Pankow, 2015; Chan and Chan, 2013; Qiu and Zhang, 2013), leading to the
56 formation of secondary organic aerosols (SOA) that aggravate air quality and
57 visibility. Gaseous amines and their oxidization products, such as nitrosamines, pose
58 significant risks to human health (Li et al., 2019a; Lee and Wexler, 2013). The
59 multiphase chemistry of atmospheric amines participates in and accelerates new
60 particle formation (Liu et al., 2022; Huang et al., 2022; Yao et al., 2018; Shen et al.,
61 2019), enhances aerosol hygroscopicity (Chu et al., 2015; Gomez-Hernandez et al.,
62 2016), and promotes the activation of cloud condensation nuclei (Tang et al., 2014;
63 Corral et al., 2022; Gomez-Hernandez et al., 2016). Additionally, amines can promote
64 the formation of brown carbon (Marrero-Ortiz et al., 2018; Lin et al., 2015), thereby
65 affecting atmospheric radiation and climate.



66 Atmospheric amines originate from diverse natural sources (e.g. ocean, soil, and
67 vegetation) and anthropogenic sources (e.g. animal husbandry, biomass burning, coal
68 combustion, vehicle emissions, composting, waste incineration, industrial activities,
69 and sewage) (Shen et al., 2017; Hemmilä et al., 2018; Feng et al., 2022). The ocean is
70 an important natural source of low molecular weight amines, with emissions mainly
71 driven by biological processes (Calderón et al., 2007; Wang and Lee, 1994). Global
72 modeling (Myriokefalitakis et al., 2010) suggested that amines contribute ~20% of
73 marine SOA, ranking second to dimethylsulfide (DMS). Amines exhibit varying
74 concentrations across different oceans in both seawater and the atmosphere (Violaki
75 and Mihalopoulos, 2010; Gibb et al., 1999; Van Neste et al., 1987). Elevated
76 concentrations of DMA and TMA are associated with biological activities (Carpenter
77 et al., 2012; Welsh, 2000) and algal blooms (Müller et al., 2009; Facchini et al.,
78 2008b). Marine organisms act as both sources and sinks of amines, and the
79 source/sink capability of the ocean varies with ambient conditions (Pinxteren et al.,
80 2019). For instance, TMA can be released from living tissues or during
81 biodegradation and decay, and can also be utilized by microorganisms for energy
82 metabolism (Sun et al., 2019; Köllner et al., 2017; Lidbury et al., 2015). TMA can be
83 biologically oxidized to trimethylamine oxide (TMAO), an osmotic regulatory
84 compound in marine organisms and a precursor of DMA and MA (Chen et al., 2011;
85 Lidbury et al., 2017). The calculated sea-to-air fluxes of DMA at Cape Verde were
86 both positive and negative, whereas those of MA were mostly positive (Pinxteren et
87 al., 2019). Amines in marine aerosols can originate from sea spray (Bates et al., 2012;
88 Gorzelska and Galloway, 1990), bubble bursting (Milne and Zika, 1993), and
89 gas-to-particle conversion through secondary formation (Rinaldi et al., 2010; Facchini
90 et al., 2008b; Facchini et al., 2008a). Most low molecular weight amines in marine



91 aerosols were considered to be secondarily formed (Gaston et al., 2013; Dall’osto et
92 al., 2019). For instance, 11–25% of MA, DMA and TMA in the Antarctic sympagic
93 environment originated from primary marine aerosols, whereas 75–89% were
94 incorporated into aerosols after air-sea exchange (Dall’osto et al., 2019). Amines in
95 marine aerosols may also be influenced by inland sources and long-range atmospheric
96 transport (Nielsen et al., 2012). TMA detected in aerosols off the coast of California
97 was associated with inland animal husbandry activities rather than local marine
98 biogenic emissions (Gaston et al., 2013).

99 Atmospheric low molecular weight amines have been widely reported in urban
100 (Cheng et al., 2020; Chen et al., 2019; Liu et al., 2017), rural (Cheng et al., 2018; Lin
101 et al., 2017), and coastal areas (Liu et al., 2022; Hu et al., 2015; Zhou et al., 2019), but
102 relatively few studies have focused on marine regions of China (Zhou et al., 2019; Yu
103 et al., 2016; Hu et al., 2015). The Bohai Sea (BS) and Yellow Sea (YS) are two
104 marginal seas in eastern China that serve as transition zones for atmospheric
105 pollutants and particles transported from East Asia to the Northwest Pacific Ocean
106 (NWPO). The BS is the northernmost marginal sea of China, surrounded by land on
107 three sides and bordered to the east by the YS. The YS is divided into North Yellow
108 Sea (NYS) and South Yellow Sea (SYS), both semi-open sea areas of the NWPO.
109 Aerosols over the YS–BS are significantly influenced by the transport of terrestrial
110 emissions from northern and eastern China during the prevailing spring East Asia
111 monsoon (Fang et al., 2016). Previous studies on amines in marine aerosols have
112 mainly focused on DMA and TMDEA (the sum of TMA and DEA) (Zhou et al., 2019;
113 Xie et al., 2018; Yu et al., 2016; Hu et al., 2015). MA has been observed as the
114 dominant amine in urban aerosols in northern China and the Yangtze River Delta
115 region (Yang et al., 2023; Liu et al., 2023). The compositions, sources, and secondary



116 formation pathways of amines in offshore aerosols of China remain unclear due to the
117 combined influence of complex terrestrial and marine emissions. Here, spatial
118 variations of amines in aerosols over the YS–BS were investigated through integrated
119 observations of 6 major amines and > 100 other chemical components during a
120 research cruise conducted in spring 2018. The potential sources and secondary
121 formation pathways of different amines were further discussed. The results will
122 enhance understanding of amines in marine aerosols, provide insights into the impact
123 of terrestrial emissions on the atmosphere over the NWPO, and support further
124 research on the gas-to-particle conversion of amines under varying ambient
125 conditions.

126

127 **2 Methods**

128 **2.1 Aerosol sampling**

129 During a Chinese oceanographic cruise over the YS–BS (28 March–16 April 2018),
130 total suspended particles (TSP) were collected on prebaked (450 °C for 6 h) quartz
131 fiber filters using a high-volume air sampler (ASM-1000, Guangzhou; flow rate: 1 m³
132 min⁻¹) aboard the *Dong Fang Hong 2* (Figure S1). The sampler was installed
133 windward on the upper deck at the ship bow (~10 m above the sea surface). To avoid
134 contamination from the ship exhaust, sampling was performed only while the vessel
135 was underway. During the sampling period, a total of 15 samples were collected, and
136 3 field blank filters were prepared by collecting without airflow. The samples were
137 categorized as SYS, NYS, and BS by sampling positions. Real-time navigation and
138 meteorological data, including position, ambient temperature (T), relative humidity
139 (RH), and wind speed (Table S1), were recorded by the onboard monitoring system.



140

141 2.2 Chemical analysis

142 Low molecular weight amines can be directly separated and quantified using ion
143 chromatography methods (Feng et al., 2020; Place et al., 2017; VandenBoer et al.,
144 2012; Gibb et al., 1995). 6 major protonated amine species, including methylamine
145 (MA), ethylamine (EA), dimethylamine (DMA), iso-propanamine (IPA), propanamine
146 (PA), and the combined species “trimethylamine (TMA) + diethylamine (DEA)”
147 (TMDEA), were measured by a Thermo Fisher Scientific Dionex ICS-5000+ system,
148 as described in detail elsewhere (Yang et al., 2023). Before analysis, a 0.8 cm^2 portion
149 of each sample or blank filter was ultrasonically extracted 3 times with 10–30 mL of
150 ultrapure water for 15 min in an ice-water bath, followed by filtration through a $0.22\text{ }\mu\text{m}$
151 Teflon filter. The analytical precision was better than 10%, and recoveries for all
152 amines ranged from 90% to 110%. The method detection limits (MDLs) for MA, EA,
153 DMA, IPA, PA, and TMDEA were 0.4 ng m^{-3} , 0.4 ng m^{-3} , 0.5 ng m^{-3} , 0.7 ng m^{-3} , 1.1
154 ng m^{-3} , and 2.9 ng m^{-3} , respectively.

155 To provide a comprehensive characterization, other key chemical components were
156 also analyzed, including water-soluble inorganic ions (WSIIs; Na^+ , NH_4^+ , K^+ , Mg^{2+} ,
157 Ca^{2+} , Cl^- , NO_3^- , SO_4^{2-} , etc.), low molecular weight organic acids (CHO_2^- , $\text{C}_2\text{H}_3\text{O}_2^-$,
158 $\text{C}_4\text{H}_4\text{O}_4^{2-}$, $\text{C}_5\text{H}_6\text{O}_4^{2-}$, $\text{CH}_3\text{O}_3\text{S}^-/\text{MSA}^-$, etc.), carbonaceous components (TC, OC, and
159 EC), and organic compositions (polar and nonpolar). Detailed methodologies had been
160 described elsewhere (Fan et al., 2019; Cao et al., 2024), and the measurement results
161 were summarized in Table S2.

162



163 **2.3 Auxiliary data**

164 Average chlorophyll *a* (Chl *a*) concentrations in seawater during the sampling period
165 were retrieved from combined Aqua-MODIS and Terra-MODIS datasets
166 (<https://oceancolor.gsfc.nasa.gov/>) using ArcGIS software (Figure S2). Fire spot
167 information was obtained from the Fire Information for Resource Management
168 System (FIRMS, <https://firms.modaps.eosdis.nasa.gov/>). Based on the archived
169 Global Data Assimilation System (<ftp://arlftp.arlhq.noaa.gov/pub/archives/gdas1/>)
170 meteorological data, 48 h backward air-mass trajectories at 200 m above ground level
171 were calculated using the Hybrid Single-particle Lagrangian Integrated Trajectory
172 (HYSPLOT) model, and subsequently processed with TrajStat software (Figure S3).

173

174 **3 Results and discussion**

175 **3.1 Overview of amines in marine aerosols**

176 During the research cruise over the YS–BS from 28 March to 16 April 2018, total
177 concentrations of MA, EA, DMA, IPA, PA, and TMDEA (Σ amines) in TSP ranged
178 from 16.2 ng m⁻³ to 89.1 ng m⁻³ (Figure 1). Lower Σ amines concentrations were
179 observed over the SYS and NYS, averaging 40.4 ± 16.4 ng m⁻³ and 43.5 ± 17.5 ng
180 m⁻³, respectively, and higher concentrations occurred over the BS, averaging 63.6 ±
181 18.3 ng m⁻³. Concentrations of other chemical components, including total WSIs, TC,
182 and total measured organic compositions, exhibited a similar spatial pattern (SYS <
183 NYS < BS; Table S2).

184 TMDEA was the predominant amine species in TSP over the YS–BS, with
185 concentrations ranging from 6.1 ng m⁻³ to 36.3 ng m⁻³ (Figure S4) and averages of
186 20.7 ± 9.1 ng m⁻³, 17.8 ± 7.3 ng m⁻³ and 23.8 ± 3.7 ng m⁻³ over the SYS, NYS and



187 BS, respectively. TMDEA accounted for a larger fraction of Σ amines over the SYS
 188 (51.2%) than the NYS (40.8%) and BS (37.4%). Compared with previous studies
 189 (Table. S3), the average TMDEA concentration in TSP over the YS–BS during
 190 March–April 2018 ($20.7 \pm 8.2 \text{ ng m}^{-3}$) was comparable to values reported for
 191 $\text{PM}_{0.056-10}$ during June–July 2016 (21.0 ng m^{-3}) and August 2015 (18.6 ng m^{-3}) (Xie
 192 et al., 2018), for $\text{PM}_{2.5}$ during January–February 2018 at coastal Qingdao (a port city
 193 surrounded by the YS and BS, 19.3 ng m^{-3}) (Liu et al., 2022), and for PM_1 in July
 194 2007 off the central coast of California, USA (22.0 ng m^{-3}) (Sorooshian et al., 2009).
 195 These values were higher than those measured in $\text{PM}_{0.056-10}$ at coastal Qingdao (9.0
 196 ng m^{-3}) (Xie et al., 2018) and in $\text{PM}_{2.5}$ at Huaniao Island (an adjacent island of China,
 197 8.7 ng m^{-3}) (Zhou et al., 2019) during August 2016, and markedly higher than those
 198 in aerosols from other marine regions, including the Arabian Sea (Gibb et al., 1999),
 199 the East Mediterranean (Violaki and Mihalopoulos, 2010), the North Atlantic
 200 (Facchini et al., 2008a), and the tropical Atlantic (Pinxteren et al., 2019; Müller et al.,
 201 2009). In aerosols over the SYS and NYS–BS, TMDEA concentrations in TSP during
 202 spring (20.7 ng m^{-3} and 20.8 ng m^{-3} in March–April 2018) were lower than those
 203 measured in PM_{10} during summer (45.6 ng m^{-3} in August 2015 and 28.8 ng m^{-3} in
 204 August–September 2015) (Yu et al., 2016).
 205 MA, the second most abundant amine species (range: $0.9\text{--}44.0 \text{ ng m}^{-3}$), exhibited
 206 average concentrations of $22.8 \pm 15.0 \text{ ng m}^{-3}$ and $15.7 \pm 7.7 \text{ ng m}^{-3}$ in TSP over the
 207 BS and NYS, contributing 35.9% to Σ amines. Relatively lower MA concentrations
 208 ($10.0 \pm 7.0 \text{ ng m}^{-3}$) and a smaller proportion of MA to Σ amines (24.9%) were
 209 observed over the SYS compared with the NYS–BS. The spatial pattern of MA
 210 contributions to Σ amines was opposite to that of TMDEA. The average MA
 211 concentration in TSP over the YS–BS ($13.7 \pm 10.5 \text{ ng m}^{-3}$) was higher than those



observed in $PM_{2.5}$ at coastal Qingdao (8.5 ng m^{-3} , winter 2018) (Liu et al., 2022), in $PM_{0.9}$ over the Arabian Sea ($3.2\text{--}3.7 \text{ ng m}^{-3}$) (Gibb et al., 1999), and in PM_1 over the tropical Atlantic (0.2 ng m^{-3}) (Pinxteren et al., 2019), but comparable to that in $PM_{2.5}$ at Jeju Island, South Korea (13.5 ng m^{-3}) (Yang et al., 2004).

DMA concentrations ranged from 1.3 ng m^{-3} to 10.4 ng m^{-3} , with averages of $3.5 \pm 2.1 \text{ ng m}^{-3}$, $3.8 \pm 2.6 \text{ ng m}^{-3}$, and $7.9 \pm 2.1 \text{ ng m}^{-3}$ in TSP over the SYS, NYS, and BS, respectively. Higher DMA contributions to Σamines were found over the BS (12.4%) than the NYS (8.7%) and SYS (8.6%). DMA concentrations in aerosols during spring 2018 over the YS–BS ($4.4 \pm 2.8 \text{ ng m}^{-3}$) were markedly lower than those observed in winter 2018 at coastal Qingdao (58.7 ng m^{-3}) (Liu et al., 2022), in summer 2015/2016 over the YS–BS (23.9 ng m^{-3} and 50.6 ng m^{-3}) (Xie et al., 2018), and in winter 2013 over the SYS (19.8 ng m^{-3}) (Yu et al., 2016). EA ($0.6\text{--}4.8 \text{ ng m}^{-3}$), IPA ($0.5\text{--}3.9 \text{ ng m}^{-3}$), and PA ($1.3\text{--}5.1 \text{ ng m}^{-3}$) constituted a relatively small fraction of Σamines (7.3–28.2%), with average concentrations of $2.0 \pm 1.2 \text{ ng m}^{-3}$, $1.8 \pm 1.0 \text{ ng m}^{-3}$, and $2.9 \pm 1.0 \text{ ng m}^{-3}$ in TSP over the YS–BS, respectively. EA concentrations in aerosols over the BS ($3.0 \pm 1.3 \text{ ng m}^{-3}$, March–April 2018) were comparable to those in $PM_{2.5}$ at coastal Qingdao (2.7 ng m^{-3} , January–February 2018) (Liu et al., 2022) and at Jeju Island, South Korea (3.1 ng m^{-3} , March–April 2001) (Yang et al., 2004). Comparable data for EA, IPA and PA concentrations in marine aerosols were currently limited. Strong positive correlations were observed among MA, EA, and DMA ($R = 0.73\text{--}0.77$, $P < 0.01$), whereas no statistically significant correlation ($P > 0.05$) exhibited between IPA, PA or TMDEA and other amine species. These results suggest that MA, EA, and DMA shared similar sources and secondary formation pathways, whereas IPA, PA, and TMDEA likely originated from different sources or undergo distinct atmospheric formation processes.



237

238 3.2 Relative contributions of amines in TSP over the YS–BS

239 Amines, as a subset of water-soluble organic carbon, generally constitute a small
 240 fraction of OC. Both OC and EC concentrations in TSP decreased significantly from
 241 the BS to the NYS and SYS (Figure 2). Higher OC/EC ratios were observed in
 242 samples from the SYS (9.8 ± 2.3), which were more strongly influenced by marine air
 243 masses (Figure S3), compared with the BS–NYS (7.9 ± 1.4 ; Figure S5). The high
 244 OC/EC ratios related to reduced contributions from terrestrial combustion sources and
 245 enhanced OC emissions from marine microorganisms. The $\sum \text{amines-C/OC}$ ratios
 246 ranged from 2.1‰ to 8.8‰, with an average of 4.9 ± 2.1 ‰ in TSP over the YS–BS.
 247 These ratios were relatively higher in aerosols over the SYS (5.4 ± 2.2 ‰) than the
 248 NYS (4.4 ± 1.7 ‰) and BS (4.0 ± 1.4 ‰).

249 Low molecular weight amines can act as strong bases even in the presence of NH_3
 250 (Sorooshian et al., 2008). They share similar emission sources and gas-to-particle
 251 conversion pathways to some extent, as indicated by the correlations between NH_4^+
 252 and MA ($R = 0.78$, $P < 0.01$), DMA ($R = 0.74$, $P < 0.01$), EA ($R = 0.57$, $P < 0.05$), PA
 253 ($R = 0.58$, $P < 0.05$), and TMDEA ($R = 0.52$, $P < 0.05$). The molar ratios of amines to
 254 NH_4^+ were calculated to evaluate their relative contributions to the neutralization of
 255 acidic species in aerosols (Hu et al., 2015). The $\sum \text{amines}/\text{NH}_4^+$ molar ratios ranged
 256 from 4.8‰ to 17.0‰ (8.7 ± 3.0 ‰) in TSP over the YS–BS, and were 9.7 ± 3.4 ‰, 7.6
 257 ± 0.8 ‰, and 6.8 ± 1.8 ‰ over the SYS, NYS, and BS, respectively. The spatial pattern
 258 of $\sum \text{amines}/\text{NH}_4^+$ molar ratios ($\text{SYS} > \text{NYS} > \text{BS}$) was consistent with that of the
 259 $\sum \text{amines-C/OC}$ ratios, indicating a north-to-south enhancement in the relative
 260 contributions of amines to aerosol composition over the YS–BS.



261 The $\sum \text{amines}/\text{NH}_4^+$ molar ratios calculated in this study were of the same order of
 262 magnitude as those reported previously (Xie et al., 2018; Yu et al., 2016). Overall,
 263 amines yield a negligible contribution to the neutralization of acidic species in TSP
 264 compared to NH_4^+ , which is reasonable given the much higher atmospheric
 265 concentrations of NH_3 relative to gaseous amines (Zheng et al., 2015; You et al., 2014;
 266 Ge et al., 2011a, b). However, amines may play a more important role in neutralizing
 267 acidic species in submicron particles, particularly in the presence of organic
 268 compounds, as suggested by the size-dependent amines/ NH_4^+ ratio hypothesis
 269 ($\text{amines}/\text{NH}_4^+_{\text{OP-LW}} \gg \text{amines}/\text{NH}_4^+_{\text{OP-WP}} > \text{amines}/\text{NH}_4^+_{\text{WP or SP}}$) (Xie et al., 2018).
 270 The secondary formation of SNA (NH_4^+ , NO_3^- , and SO_4^{2-}) interacts with that of
 271 amines, thereby influencing their concentrations and compositions in aerosols. The
 272 $\text{NH}_4^+/(\text{Cl}^- + \text{NO}_3^- + 2 \times \text{SO}_4^{2-})$ molar ratios in TSP over the YS–BS were mostly < 1
 273 (0.8 ± 0.2 ; Figure 2 and Figure S5), indicating NH_4^+ deficiency in aerosols, and the
 274 NH_4^+ deficiency was more markedly over the BS (0.6 ± 0.0) than the YS (0.8 ± 0.2).
 275 The $\text{NO}_3^-/\text{SO}_4^{2-}$ molar ratios in TSP over the SYS were 0.8 ± 0.8 , significantly lower
 276 than those over the NYS (2.3 ± 0.4) and BS (2.5 ± 0.8), suggesting that SO_4^{2-} was the
 277 dominate acidic species in SYS aerosols, whereas NO_3^- dominated in NYS and BS
 278 aerosols. The characteristics of SNA in NYS aerosols were intermediate between
 279 those over the BS and SYS, consistent with the regional variations in concentrations
 280 and compositions of amines. Molar concentrations of $\sum \text{amines}$ increased with the
 281 NH_4^+ deficiency [indicated by $\text{NH}_4^+/(\text{Cl}^- + \text{NO}_3^- + 2 \times \text{SO}_4^{2-})$ ratios; $R = -0.57$, $P <$
 282 0.05] and with the $\text{NO}_3^-/\text{SO}_4^{2-}$ ratios ($R = 0.56$, $P < 0.05$), particularly in BS aerosols.
 283 Nevertheless, individual amines responded differently to variations in NH_4^+
 284 deficiency and $\text{NO}_3^-/\text{SO}_4^{2-}$ molar ratios, reflecting their distinct emission sources and
 285 formation mechanisms.



286

287 **3.3 Source analysis of amines in TSP over the YS–BS**

288 **3.3.1 Biogenic sources**

289 On a global scale, the ocean is a major source of gaseous methylamines (fluxes: TMA >
 290 MA >> DMA) (Van Neste et al., 1987; Schade and Crutzen, 1995). Intensive ocean
 291 farming is widespread in the coastal areas of the YS–BS (Hu et al., 2015), where
 292 marine biogenic sources, including fish emission (Namieśnik et al., 2003),
 293 biodegradation of nitrogen-containing materials, and decay process (Calderón et al.,
 294 2007) may release gaseous amines into the atmosphere. The concentration of Chl *a* in
 295 surface seawater is an indicator of phytoplankton biomass and thus reflects the
 296 intensity of marine biogenic emissions to some extent. Significantly higher Chl *a*
 297 concentrations were observed in the BS than in the YS, with relatively elevated values
 298 in near shore areas (Figure S2). The spatial distribution of Σ amines in TSP over the
 299 YS–BS was broadly consistent with, though not identical to, the Chl *a* concentrations
 300 in surface seawater. This was attributed to secondary formation processes of amines
 301 in aerosols, as well as the influence of long-range transport of terrestrial emissions
 302 driven by the prevailing East-Asia monsoon during spring, particularly to S10, S12,
 303 and S14–18 (Figure S3).

304 MA, EA, and DMA exhibited positive linear relationships with the total
 305 concentrations of primary sugars and sugar alcohols (Figure 3 a–c and Table S4),
 306 which mainly originate from primary biogenic sources such as bacteria, pollen, and
 307 animal or plant debris (Li et al., 2019b). These primary biogenic sources can be either
 308 marine or terrestrial. Fungal spore OC and plant debris OC were estimated from the
 309 concentrations of mannitol and arabitol (Bauer et al., 2008), and glucose (Zheng et al.,



2018), respectively. Significant positive correlations were observed between MA, EA, and DMA and fungal spore OC, plant debris OC, and several individual primary sugars and sugar alcohols, including trehalose, α -fructose, and sucrose ($R > 0.50$, $P < 0.05$). DMA exhibited the strongest correlation with trehalose ($R = 0.71$, $P < 0.01$), which is abundant in microorganisms, algae, plants, and invertebrates, and also acts as an indicator of re-suspended dust (Medeiros et al., 2006; Simoneit et al., 2004). In addition, MA, DMA, and PA were correlated with high molecular weight *n*-alkanes (ALK_{HMW} ; C_{27} , C_{29} , C_{31} and C_{33}) and high molecular weight fatty alcohols (ALC_{HMW} ; $> C_{19alc}$; Figure 3 d–e and Table S4). ALK_{HMW} (Rogge et al., 1993), ALC_{HMW} (Simoneit et al., 1991), and high molecular weight fatty acids (FA_{HMW} , $> C_{19:0}$) (Haque et al., 2019) are tracers of higher plant waxes, emitted by terrestrial vegetation. A significant positive relationship was also observed between PA and low molecular weight fatty acids (FA_{LMW} ; $\leq C_{19:0}$; Figure 3 f), which can be emitted by microorganisms, phytoplankton, or bacteria (Haque et al., 2019) and are considered tracers of marine/microbial sources in marine aerosols. These results indicate that amines (MA, EA, DMA, and PA) in TSP over the YS–BS were contributed by biogenic sources. MA and DMA were largely influenced by terrestrial biogenic emissions, whereas PA was affected by both terrestrial and marine biogenic sources.

Atmospheric biogenic secondary organic aerosols (BSOA) are formed through the photochemical oxidation of biogenic volatile organic compounds (BVOCs) with O_3 , OH and NO_x (Ng et al., 2011). 6 isoprene SOA (SOA_I) tracers, 3 monoterpene SOA (SOA_M) tracers, and 1 β -caryophyllene SOA (SOA_C) tracer were measured in TSP over the YS–BS. Biogenic SOC derived from isoprene, monoterpene, and β -caryophyllene was estimated using the tracer-based method (Kang et al., 2018; Kleindienst et al., 2007). Significant positive linearity were observed between MA



335 and both isoprene SOC and monoterpene SOC (Figure 3 g–h). Among the 6 SOA_I
 336 tracers, MA exhibited stronger correlations with 2-methyltetrols (2-MTLs; $R = 0.74$, P
 337 < 0.01) and C₅-alkene triols ($R = 0.66$, $P < 0.01$) than with 2-methylglyceric acid
 338 (2-MGA; $R = 0.64$, $P < 0.05$). DMA also showed a positive correlation with isoprene
 339 SOC ($R = 0.55$, $P < 0.05$), only driven by its association with 2-MTLs ($R = 0.59$, $P <$
 340 0.05). Among the 3 SOA_M tracers, significant correlations were found between
 341 pinonic acid and MA ($R = 0.73$, $P < 0.01$), EA ($R = 0.52$, $P < 0.05$), and DMA ($R =$
 342 0.58 , $P < 0.05$), as well as between pinic acid with MA ($R = 0.59$, $P < 0.05$). In
 343 addition, a positive linearity was observed between only PA and β -caryophyllene SOC
 344 ($R = 0.67$, $P < 0.01$; Figure 3 i). These findings supported that MA, EA, DMA and PA
 345 shared common emission sources with BSOA precursors and/or interact with BSOA
 346 formation processes. High concentrations of amines and biomarkers were
 347 simultaneously observed in the BS and NYS aerosols, and amines in SYS aerosols
 348 reached moderate levels even under low biomarker concentrations (Figure 3). These
 349 indicated that terrestrial biogenic emissions contributed more substantially to amines
 350 in aerosols over the BS and NYS than the SYS.

351

352 3.3.2 Anthropogenic sources

353 Anthropogenic sources were another important potential contributor to atmospheric
 354 amines. These sources can be categorized into combustion-related sources (e.g.,
 355 biomass burning, coal combustion, vehicle emissions, and waste incineration) and
 356 non-combustion sources (e.g., animal husbandry, composting, industrial activities,
 357 sewage, and septic system). The concentrations of EA ($R = 0.61$, $P < 0.05$) and DMA
 358 ($R = 0.72$, $P < 0.01$) in TSP over the YS–BS showed synchronous increases with EC,



359 indicating the influence of combustion emissions. Levoglucosan (Lev) is a
 360 well-established tracer for biomass burning (Li et al., 2019b). The concentrations of
 361 Lev derived from biomass burning (Lev_{bb}) were estimated using Lev and non-sea-salt
 362 K^+ ($\text{nss-K}^+ = \text{K}^+ - 0.037 \times \text{Na}^+$), considering the atmospheric degradation of Lev and
 363 that ~25% of Lev originated from other sources [$\text{Lev}_{\text{bb}} = 0.75 \times \text{Lev} \times \text{nss-K}^+ / (0.18 \times$
 364 $\text{Lev} + 0.08 \times \text{nss-K}^+)$]. Biomass burning was not a major source of MA, EA, and
 365 DMA in marine aerosols (Figure 3 j), but it contributed substantially to PA, as
 366 indicated by the positive linear relationships between PA and both Lev_{bb} and lignin
 367 products (Figure 3 k–l). The most significant contributor to PA from biomass burning
 368 might be conifer burning (the second-largest portion of total biomass burning),
 369 according to the correlations of PA and individual lignin products: 4-hydroxybenzoic
 370 acid (4-HBA; a herbs burning marker and the dominate lignin product in this study; R
 371 $= 0.52$, $P < 0.05$), vanillic acid (VA; a softwood and hardwood burning marker; R
 372 $= 0.67$, $P < 0.01$), syringic acid (SA; also a softwood and hardwood burning marker; R
 373 $= 0.60$, $P < 0.05$), and dehydroabietic acid (DA; a conifer burning marker; $R = 0.71$, P
 374 < 0.01). MA ($R = 0.57$, $P < 0.05$) and DMA ($R = 0.54$, $P < 0.05$) in TSP over the
 375 YS–BS exhibited positive correlations with polycyclic aromatic hydrocarbons (PAHs),
 376 suggesting potential contributions from fossil fuel combustion (Table S4). PA showed
 377 a stronger association with combustion-related sources than other amines, as
 378 evidenced by its correlations with multiple fossil fuel combustion tracers (Figure 3
 379 m–o), including low molecular weight n-alkanes (ALK_{LMW} ; $\text{C}_{20}\text{--}\text{C}_{26}$; $R = 0.67$, $P <$
 380 0.01), PAHs ($R = 0.63$, $P < 0.05$), hopanes ($R = 0.55$, $P < 0.05$), and steranes ($R = 0.57$,
 381 $P < 0.05$).
 382 Emissions of amines (MA, DMA, and TMA) from non-combustion anthropogenic
 383 sources, such as composting, sewage, and septic system, are largely linked to



384 biodegradation process. Therefore, the contribution of non-combustion anthropogenic
 385 sources to amines might be encompassed within the primary biogenic sources
 386 category. IPA did not show any correlation with organic molecular tracers in TSP over
 387 the YS–BS. Given its widespread use in industrial production (e.g., pesticides,
 388 pharmaceuticals, dye intermediates, emulsifiers, detergents, surfactants, and textile
 389 additives), IPA might be emitted in particulate form from specific industrial activities
 390 (Ge et al., 2011b).

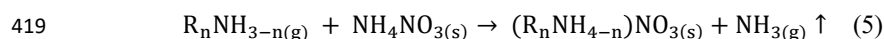
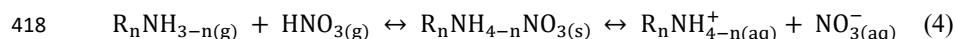
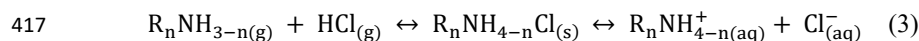
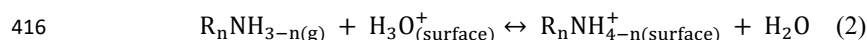
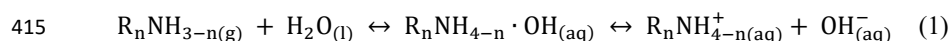
391

392 **3.3.3 Secondary formation of MA, EA, DMA, and PA**

393 Significant correlations were observed between MA, EA, DMA, and PA with Cl^- and
 394 NO_3^- (Figure 4). The intercepts of the regression lines for MA, EA, and DMA against
 395 Cl^- or NO_3^- were lower than those obtained with organic molecular tracers of primary
 396 sources (Figure 3 and Figure S6), indicating the substantial contribution from
 397 secondary formation. Direct dissolution of gaseous amines into aerosol liquid water
 398 (Formula 1) is a key step in the gas-to-particle conversion of MA (CH_3NH_2), EA
 399 ($\text{CH}_3\text{CH}_2\text{NH}_2$), and DMA [$(\text{CH}_3)_2\text{NH}$], all of which are highly water-soluble. Low T,
 400 high aerosol acidity, and high atmospheric liquid water content favor this process.
 401 Gaseous amines may also undergo directly uptake onto acidic particle surfaces
 402 (Formula 2) (Yin et al., 2011), which is particularly important under the NH_4^+
 403 deficiency observed in BS aerosols. Acid-base reactions between amines and
 404 inorganic acids occur in both gas and aqueous phases. Protonated amines (aminium
 405 salts), including MA (CH_3NH_3^+), EA ($\text{CH}_3\text{CH}_2\text{NH}_3^+$), DMA [$(\text{CH}_3)_2\text{NH}_2^+$], and PA
 406 ($\text{CH}_3\text{CH}_2\text{CH}_2\text{NH}_3^+$), in TSP over the YS–BS could be formed through reactions with
 407 atmospheric HCl and HNO_3 (Formula 3–4). Atmospheric CH_3COOH also contributed



408 to the formation of MA, EA and DMA in TSP (Figure 4). As NO_3^- concentrations
 409 were significantly higher than those of Cl^- and $\text{C}_2\text{H}_3\text{O}_2^-$ in TSP (Table S2), reactions
 410 with HNO_3 , along with displacement reactions between gaseous amines and NH_4NO_3
 411 (Formula 5) (Bzdek et al., 2010), were the dominate pathway for the secondary
 412 formation of MA, EA, DMA and PA in TSP over the YS–BS. The partitioning of
 413 amines into aerosols was further promoted by low T, high aerosol acidity, and high
 414 RH conditions in the dynamic solid/aqueous/gas equilibrium.



420 Nitrate-associated secondary formation contributions were estimated from the average
 421 amines concentrations weighted by NO_3^- concentrations and the regression intercepts
 422 (Figure S6). These contributions to \sum amines in TSP were highest over the BS (43.0%),
 423 followed by the NYS (33.8%) and SYS (21.8%). Among individual amines,
 424 nitrate-associated secondary formation contributed most to MA (BS: 79.3%; NYS:
 425 70.5%; SYS: 57.2%), followed by DMA (BS: 73.3%; NYS: 48.3%; SYS: 55.5%), EA
 426 (BS: 61.2%; NYS: 47.2%; SYS: 29.0%), and PA (BS: 41.1%; NYS: 30.5%; SYS:
 427 25.2%). PA might also be directly emitted in particulate form or condense into
 428 aerosols after emission due to its relatively higher boiling point (47.8°C) compared
 429 with MA (−6.3°C), EA (16.6°C), and DMA (7.4°C).

430 Interactions might exist among the secondary formation of amines (MA, EA, DMA,
 431 and PA), BSOA, and nitrate in the atmosphere. NO_x , emitted by soil, biogenic



activities, and combustion sources, are important precursors for both BSOA and atmospheric HNO_3 , which subsequently forms nitrate aerosols. These were supported by the significant positive correlations between NO_3^- and SOA_I ($R = 0.88$, $P < 0.01$), SOA_M ($R = 0.86$, $P < 0.01$), and SOA_C ($R = 0.64$, $P < 0.05$). The formation of MA and DMA in aerosols could occur under low NO_x conditions, as evidenced by their stronger correlations (Text S1) with 2-MTLs or C_5 -alkene triols (products of isoprene photochemical oxidation under low NO_x conditions) (Zheng et al., 2018; Zhang et al., 2011) than with 2-MGA (products of isoprene aqueous-phase oxidation under high NO_x conditions) (He et al., 2018). Strong atmospheric photo-oxidation conditions generally accelerates the gas-phase degradation of amines (Lee and Wexler, 2013) due to their reactions with OH, O_3 and NO_x [nitrate radical (NO_3) and HONO ($\text{HONO} \leftrightarrow \text{NO} + \text{NO}_2 + \text{H}_2\text{O}$)], thereby reducing the formation of particle-phase aminium salts. BVOCs, precursors of BSOA, generated HNO_3 via the “ $\text{NO}_3 + \text{HC}$ ” pathway, further enhancing the formation of aminium nitrates. Meanwhile, BSOA formation consumed atmospheric oxidants, which reduced the degradation of gaseous amines to some extent. The presence of an organic phase also increased the competitiveness of amines relative to NH_4^+ in aerosols (Xie et al., 2018). In addition, the gas-to-particle conversion of amines promoted particle nucleation and growth, providing more hygroscopic particulate surfaces that facilitate further BSOA formation.

During the cruise, lower average T and RH were observed over the BS (9.0°C , 67.2%) and NYS (6.7°C , 85.7%) compared to the SYS (9.5°C , 91.8%). RH over the YS–BS generally (90%) remained at a high level ($> 61.1\%$, median: 87.6%). The relatively abundant acidic species and lower T over the BS and NYS favored the partitioning of MA, EA, DMA, and PA into the particle phase, compared with the conditions over the SYS.



457

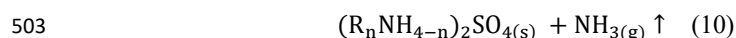
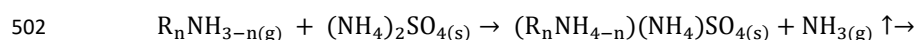
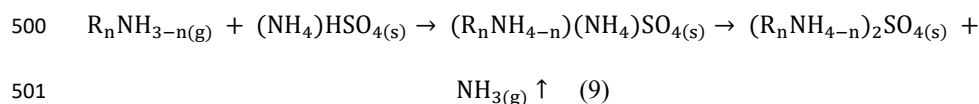
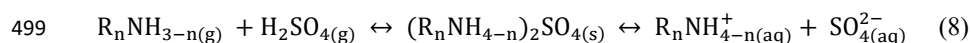
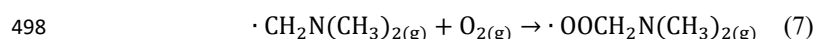
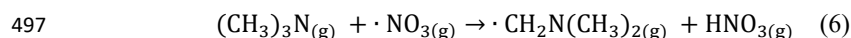
458 **3.3.4 Secondary formation of TMDEA**

459 TMDEA in TSP over the YS–BS showed no correlation with the measured organic
 460 molecular tracers, Cl^- , or NO_3^- , but exhibited significant positive linear relationships
 461 with SO_4^{2-} , $\text{C}_4\text{H}_4\text{O}_4^{2-}$, and $\text{C}_5\text{H}_6\text{O}_4^{2-}$ (Table S4, Figure 4 and Figure S6). Compared
 462 with other amines, a larger fraction of TMDEA originated from marine sources, as
 463 suggested by its relatively high concentrations and proportions in TSP over the SYS.
 464 Previous studies reported that the global flux of TMA from the ocean was 1.6 times
 465 that of MA (Schade and Crutzen, 1995), and DEA has also been detected in seawater
 466 and marine aerosols at the tropical Atlantic (Pinxteren et al., 2019). Marine sources
 467 were an important contributor of gaseous TMDEA over the YS–BS. In addition,
 468 terrestrial vegetation and non-combustion anthropogenic sources (mainly including
 469 septic system, animal husbandry, composting, and sewage) also contributed gaseous
 470 TMDEA (Zhu et al., 2022; Ge et al., 2011b). However, the concentrations of TMDEA
 471 in aerosols were constrained by its gas-to-particle conversion efficiency.

472 Reactions between TMDEA and NO_3 lead to the formation of non-aminium-salt SOA
 473 (Price et al., 2016; Price et al., 2014). Taking TMA $[(\text{CH}_3)_3\text{N}]$ as an example, the
 474 reactions (Formula 6–7) produce HNO_3 and peroxy radicals, which subsequently
 475 undergo hydrogen rearrangement to generate particle-phase oligomers. This pathway
 476 not only yields atmospheric HNO_3 through the “ $\text{NO}_3 + \text{HC}$ ” mechanism but also
 477 consumes part of the gaseous TMDEA emitted from primary sources. Uptake onto
 478 acidic particle surfaces (Formula 2) is a key step in the gas-to-particle conversion of
 479 TMDEA, as TMA exhibits the strongest alkalinity among gaseous amines. TMDEA in
 480 TSP over the YS–BS was not inclined to present as chloride and nitrate, attributing to



the much lower competitiveness of TMA in forming chloride and nitrate (reflected by dissociation constants) relative to MA, EA, DMA, and NH₃ (Ge et al., 2011a). Instead, acid-base reactions of TMA and DEA with H₂SO₄ (Formula 8), as well as displacement reactions with (NH₄)HSO₄ and (NH₄)₂SO₄ (Formula 9–10), were the dominate pathways for the secondary formation of TMDEA in TSP over the YS–BS. These findings were consistent with previous studies that TMA had been proofed to preferentially nucleate with H₂SO₄ (Johnson and Jen, 2023), and irreversible reactive uptake of gaseous ethylamines by H₂SO₄ had been observed, with DEA exhibiting the highest uptake coefficient (Yin et al., 2011). Sulfate-associated secondary formation contributed 61.4%, 55.8%, and 63.4% (estimated by average TMDEA concentrations weighted by SO₄²⁻ concentrations and the regression intercepts, Figure S6) to TMDEA in TSP over the BS, NYS, and SYS, respectively, corresponding to 23.0%, 22.8%, and 32.5% to Σamines. These contributions increased with average T, which were higher over the SYS, followed by the BS and NYS. Dicarboxylic acids (C₄H₄O₄ and C₅H₆O₄) also contributed to the secondary formation of TMDEA in TSP over the YS–BS through reactions similar to Formula 8.



Significant positive correlations were observed between non-sea-salt sulfate



505 $(\text{nss-SO}_4^{2-} = \text{SO}_4^{2-} - 0.2516 \times \text{Na}^+)$ and the dicarboxylates $\text{C}_4\text{H}_4\text{O}_4^{2-}$ and $\text{C}_5\text{H}_6\text{O}_4^{2-}$
 506 ($R = 0.78$ and 0.66 , $P < 0.01$), indicating that these species shared similar potential
 507 terrestrial anthropogenic or marine biogenic origins (Miyazaki et al., 2010; Mochida
 508 et al., 2003). Molar concentrations of biogenic- SO_4^{2-} were estimated from T (Table
 509 S1) and MSA^- , as both MSA^- and SO_4^{2-} are oxidation products of DMS emitted from
 510 marine biogenic sources (Nakamura et al., 2005; Bates et al., 1992).
 511 Anthropogenic- SO_4^{2-} was determined by subtracting biogenic- SO_4^{2-} from nss-SO_4^{2-} .
 512 Biogenic- SO_4^{2-} accounted for 11.1% of total SO_4^{2-} in TSP over the SYS, markedly
 513 higher than the contributions over the NYS (4.3%) and BS (2.1%), yet still
 514 representing a minor fraction relative to anthropogenic- SO_4^{2-} . TMDEA in TSP over
 515 the YS–BS was predominantly taken up by anthropogenic sulfate aerosols.
 516 High concentrations of TMDEA, SO_4^{2-} , $\text{C}_4\text{H}_4\text{O}_4^{2-}$, and $\text{C}_5\text{H}_6\text{O}_4^{2-}$ were simultaneously
 517 observed in S5 and S6 over the SYS, along with relatively high marine biogenic
 518 contributions (Biogenic- $\text{SO}_4^{2-}/\text{SO}_4^{2-}$: 11.2% and 10.3%). NH_4^+ deficiency [$\text{NH}_4^+/(\text{Cl}^-$
 519 $+ \text{NO}_3^- + 2*\text{SO}_4^{2-})$: 0.8 and 0.6], high T (12.2°C and 12.1°C), high wind speed (6.9 m
 520 s^{-1} and 7.2 m s^{-1}), and saturated water vapor (RH = 100%) conditions were also found
 521 in S5 and S6 (Table S1). Under high RH conditions, more amines partition into
 522 aqueous aerosols through direct dissolution, favoring the formation of aminium salts.
 523 However, high T can shift the solid/aqueous/gas equilibrium of aminium salts toward
 524 the gas phase. In comparison with the chlorides and nitrates of MA, EA, DMA, and
 525 PA, TMDEA sulfates are more stable under high T conditions. Additionally, high wind
 526 speeds enhance the emission of primary marine aerosols from sea spray and bubble
 527 bursting, further contributing amines in TSP, as amines are present in both seawater
 528 and primary marine aerosols. The source contributions and major secondary
 529 formation pathways of amines were summarized in Figure 5.



530

531 **4 Conclusions**

532 This study presented a systematic analysis of the spatial variations, potential sources,
533 and secondary formation mechanisms of low molecular weight amines in aerosols
534 over the marginal seas of China. A consistent spatial pattern was observed for
535 concentrations of total amines, water soluble inorganic ions, carbonaceous
536 components, and > 100 organic compositions, exhibiting a north-to-south decreasing
537 trend from the BS to the NYS and SYS. This pattern was attributed to the weakening
538 influence of atmospheric pollutants transported from mainland East Asia, with the
539 increasing contribution from the marine atmosphere.

540 Offshore aerosols exhibited distinct compositions of amines compared to terrestrial
541 aerosols, with TMDEA surpassing MA as the predominant amine. The proportions of
542 TMDEA in Σ amines and the relative contributions of Σ amines in aerosols increased
543 from north to south (BS < NYS < SYS), highlighting the ocean as a substantial source
544 of amines, particularly TMDEA, despite the significant influence of terrestrial
545 emissions. MA, EA, and DMA were mainly derived from terrestrial biogenic and
546 non-combustion anthropogenic sources, followed by fossil fuel combustion, with > 50%
547 formed via nitrate-associated secondary formation pathways that interacted with
548 BSOA formation. In comparison, PA mainly originated from combustion-related
549 sources, along with terrestrial and marine biogenic sources, with a smaller fraction
550 (35%) contributed by nitrate-associated secondary formation. Different from other
551 amines, TMDEA was mostly (> 60%) generated through sulfate-associated secondary
552 formation pathways, and was also contributed from primary marine aerosols, such as
553 sea spray and bubble bursting.



554 Terrestrial sources not only release gaseous amines but also provide atmospheric
555 acidic species (e.g., SO₂ and NO_x), which participate in and accelerate new particle
556 formation. Moreover, acidic aerosols transported from the mainland can further
557 uptake gaseous amines from marine sources. These processes influence the
558 physicochemical properties and climate effects of marine aerosols, as well as the
559 carbon and nitrogen cycles. In addition to precursor abundance, ambient conditions,
560 including T, RH, and atmospheric (photo-)oxidation capacity (e.g., OH, O₃ and NO_x
561 concentrations), influence the secondary formation of amines, leading to temporal and
562 spatial variations in the concentrations and compositions of amine in aerosols. Overall,
563 these findings improve the understanding of amines in marine aerosols, highlight the
564 significant impact of terrestrial emissions on offshore aerosol chemistry, and
565 underscore the importance of multiphase chemical processes of amines under diverse
566 ambient conditions.

567

568 *Data availability.* Data are available from the corresponding author on request
569 (dryanlinzhang@outlook.com).

570

571 *Supplement.* The supplement related to this article is available online.

572

573 *Author contributions.* Xiao-Ying Yang wrote the draft and produced all the figures and
574 tables. Fang Cao, Yu-Chi Lin, and Yan-Lin Zhang provided useful comments and
575 revised the paper. Chang-Liu Wu, Yu-Xian Zhang, and Wen-Huai Song provided the
576 measurement data.

577



578 *Competing interests.* The authors declare that they have no conflict of interest.

579

580 *Acknowledgements.* We sincerely thank the captain and all crews of the *Dong Fang*
 581 *Hong 2*; Wen-shuai Li and Tian-tian Liu from the Ocean University of China for their
 582 help in the research cruise; Yi-xuan Zhang, Yan Fang, Sheng-cheng Shao, Xia Wu and
 583 Tong Huang from Nanjing University of Information Science & Technology for their
 584 assistance in the aerosol sampling and experiment process.

585

586 *Financial support.* This study was financially supported by National Natural Science
 587 Foundation of China (No. 42325304 and 41977185).

588

589 **References**

- 590 Barsanti, K., and Pankow, J.: Thermodynamics of the formation of atmospheric organic particulate
 591 matter by accretion reactions—Part 3: Carboxylic and dicarboxylic acids, *Atmospheric*
 592 *Environment*, 40, 6676-6686, <https://doi.org/10.1016/j.atmosenv.2006.03.013>, 2006.
- 593 Bates, T., Calhoun, J., and Quinn, P.: Variations in the methanesulfonate to sulfate molar ratio in
 594 marine aerosol particles over the South Pacific Ocean, *J. Geophys. Res.*, 97(D9), 9859-9865,
 595 <https://doi.org/10.1029/92JD00411>, 1992.
- 596 Bates, T. S., Quinn, P. K., Frossard, A. A., Russell, L. M., Hakala, J., Petäjä, T., Kulmala, M.,
 597 Covert, D. S., Cappa, C. D., Li, S. M., Hayden, K. L., Nuaaman, I., McLaren, R., Massoli, P.,
 598 Canagaratna, M. R., Onasch, T. B., Sueper, D., Worsnop, D. R., and Keene, W. C.: Measurements
 599 of ocean derived aerosol off the coast of California, *Journal of Geophysical Research:*
 600 *Atmospheres*, 117, n/a-n/a, <https://doi.org/10.1029/2012jd017588>, 2012.
- 601 Bauer, H., Claeys, M., Vermeylen, R., Schüller, E., Weinke, G., Berger, A., and Puxbaum, H.:
 602 Arabitol and mannitol as tracers for a quantification of airborne fungal spores, *Atmospheric*
 603 *Environment*, 42, 588-593, <https://doi.org/10.1016/j.atmosenv.2007.10.013>, 2008.
- 604 Bzdek, B., Ridge, D., and Johnston, M.: Amine exchange into ammonium bisulfate and
 605 ammonium nitrate nuclei, *Atmospheric Chemistry and Physics Discussions*, 10, 45-68,
 606 <https://doi.org/10.5194/acpd-10-45-2010>, 2010.
- 607 Calderón, S., Poor, N., and Campbell, S.: Estimation of the particle and gas scavenging



608 contributions to wet deposition of organic nitrogen, *Atmospheric Environment*, 41, 4281-4290,
 609 <https://doi.org/10.1016/j.atmosenv.2006.06.067>, 2007.

610 Cao, F., Zhang, Y.-X., Zhang, Y.-L., Song, W.-H., Zhang, Y.-X., Lin, Y.-C., Gul, C., and Haque, M.
 611 M.: Molecular compositions of marine organic aerosols over the Bohai and Yellow Seas: Influence
 612 of primary emission and secondary formation, *Atmospheric Research*, 297, 107088,
 613 <https://doi.org/10.1016/j.atmosres.2023.107088>, 2024.

614 Carpenter, L., Archer, S., and Beale, R.: Ocean-atmosphere trace gas exchange, *Chemical Society*
 615 *reviews*, 41, 6473-6506, <https://doi.org/10.1039/c2cs35121h>, 2012.

616 Chan, L., and Chan, C.: Role of the Aerosol Phase State in Ammonia/Amines Exchange Reactions,
 617 *Environmental science & technology*, 47, <https://doi.org/10.1021/es4004685>, 2013.

618 Chen, Y., Patel, N., Crombie, A., Scrivens, J., and Murrell, J.: Bacterial flavin-containing
 619 monooxygenase is trimethylamine monooxygenase, *Proceedings of the National Academy of*
 620 *Sciences of the United States of America*, 108, 17791-17796,
 621 <https://doi.org/10.1073/pnas.1112928108>, 2011.

622 Chen, Y., Tian, M., Shi, G., Wang, H., Peng, C., Cao, J., Wang, Q., Zhang, S., Guo, D., Zhang, L.,
 623 and Yang, F.: Characterization of urban amine-containing particles in southwestern China:
 624 Seasonal variation, source, and processing, *Atmospheric Chemistry and Physics*, 19, 3245-3255,
 625 <https://doi.org/10.5194/acp-19-3245-2019>, 2019.

626 Cheng, C., Huang, Z., Chan, C., Chu, Y., Li, M., Zhang, T., Ou, Y., Chen, D., Cheng, P., Lei, L.,
 627 Gao, W., Huang, Z., Huang, B., Fu, Z., and Zhou, Z.: Characteristics and mixing state of
 628 amine-containing particles at a rural site in the Pearl River Delta, China, *Atmospheric Chemistry*
 629 *and Physics*, 18, 9147-9159, <https://doi.org/10.5194/acp-18-9147-2018>, 2018.

630 Cheng, G., Hu, Y., Sun, M., Chen, Y., Chen, Y., Zong, C., Chen, J., and Ge, X.: Characteristics and
 631 potential source areas of aliphatic amines in PM_{2.5} in Yangzhou, China, *Atmospheric Pollution*
 632 *Research*, 11, 296-302, <https://doi.org/10.1016/j.apr.2019.11.002>, 2020.

633 Chu, Y., Sauerwein, M., and Chan, C. K.: Hygroscopic and phase transition properties of alkyl
 634 aminium sulfates at low relative humidities, *Physical Chemistry Chemical Physics*, 17,
 635 19789-19796, <https://doi.org/10.1039/C5CP02404H>, 2015.

636 Corral, A. F., Choi, Y., Collister, B. L., Crosbie, E., Dadashazar, H., DiGangi, J. P., Diskin, G. S.,
 637 Fenn, M., Kirschler, S., Moore, R. H., Nowak, J. B., Shook, M. A., Stahl, C. T., Shingler, T.,
 638 Thornhill, K. L., Voigt, C., Ziemba, L. D., and Sorooshian, A.: Dimethylamine in cloud water: a
 639 case study over the northwest Atlantic Ocean, *Environmental Science: Atmospheres*, 2, 1534-1550,
 640 <https://doi.org/10.1039/D2EA00117A>, 2022.

641 Dall'osto, M., Airs, R., Beale, R., Cree, C., Fitzsimons, M., Beddows, D., Harrison, R., Ceburnis,
 642 D., O'Dowd, C., Rinaldi, M., Paglione, M., Nenes, A., Decesari, S., and Simó, R.: Simultaneous
 643 Detection of Alkylamines in the Surface Ocean and Atmosphere of the Antarctic Sympagic
 644 Environment, *ACS Earth and Space Chemistry*, 3, 854-862,
 645 <https://doi.org/10.1021/acsearthspacechem.9b00028>, 2019.



646 Facchini, M., Decesari, S., Rinaldi, M., Carbone, C., Finessi, E., Mircea, M., Sandro, F., Moretti,
 647 F., Tagliavini, E., Ceburnis, D., and O'Dowd, C.: Important Source of Marine Secondary Organic
 648 Aerosol from Biogenic Amines, *Environmental science & technology*, 42, 9116-9121,
 649 <https://doi.org/10.1021/es8018385>, 2008a.

650 Facchini, M., Rinaldi, M., Decesari, S., Carbone, C., Finessi, E., Mircea, M., Sandro, F., Ceburnis,
 651 D., Flanagan, R., Nilsson, E., de Leeuw, G., Martino, M., Woeltjen, J., and Dowd, C.: Primary
 652 submicron marine aerosol dominated by insoluble organic colloids and aggregates, *Geophysical*
 653 *Research Letters*, 35, L17814, <https://doi.org/10.1029/2008GL034210>, 2008b.

654 Fan, M.-Y., Zhang, Y.-L., Lin, Y.-C., Chang, Y.-H., Cao, F., Zhang, W.-Q., Hu, Y.-B., Bao, M.-Y.,
 655 Liu, X.-Y., Zhai, X.-Y., Lin, X., Zhao, Z.-Y., and Song, W.-H.: Isotope-based source
 656 apportionment of nitrogen-containing aerosols: A case study in an industrial city in China,
 657 *Atmospheric Environment*, 212, 96-105, <https://doi.org/10.1016/j.atmosenv.2019.05.020>, 2019.

658 Fang, Y., Chen, Y., Tian, C., Lin, T., Hu, L., Li, J., and Zhang, G.: Application of PMF receptor
 659 model merging with PAHs signatures for source apportionment of black carbon in the continental
 660 shelf surface sediments of the Bohai and Yellow Seas, China, *Journal of Geophysical Research:*
 661 *Oceans*, 121, 1346-1359, <https://doi.org/10.1002/2015JC011214>, 2016.

662 Feng, H., Ye, X., Liu, Y., Wang, Z., Gao, T., Cheng, A., and Chen, J.: Simultaneous Determination
 663 of Nine Atmospheric Amines and Six Inorganic Ions by Non-suppressed Ion Chromatography
 664 Using Acetonitrile and 18-Crown-6 as Eluent Additive, *Journal of Chromatography A*, 461234,
 665 <https://doi.org/10.1016/j.chroma.2020.461234>, 2020.

666 Feng, X., Wang, C., Feng, Y., Junjie, C., Zhang, Y., Qi, X., Li, Q., Li, J., and Chen, Y.: Outbreaks
 667 of Ethyl-Amines during Haze Episodes in North China Plain: A Potential Source of Amines from
 668 Ethanol Gasoline Vehicle Emission, *Environmental Science & Technology Letters*, 9, 306-311,
 669 <https://doi.org/10.1021/acs.estlett.2c00145>, 2022.

670 Gaston, C., Quinn, P., Bates, T., Gilman, J., Bon, D., Kuster, W., and Prather, K.: The impact of
 671 shipping, agricultural, and urban emissions on single particle chemistry observed aboard the R/V
 672 Atlantis during CalNex, *Journal of Geophysical Research: Atmospheres*, 118,
 673 <https://doi.org/10.1002/jgrd.50427>, 2013.

674 Ge, X., Wexler, A., and Clegg, S.: Atmospheric amines – Part II. Thermodynamic properties and
 675 gas/particle partitioning, *Atmospheric Environment*, 45, 561-577,
 676 <https://doi.org/10.1016/j.atmosenv.2010.10.013>, 2011a.

677 Ge, X., Wexler, A., and Clegg, S.: Atmospheric amines – Part I. A review, *Atmospheric*
 678 *Environment*, 45, 524-546, <https://doi.org/10.1016/j.atmosenv.2010.10.012>, 2011b.

679 Gibb, S., Mantoura, R. F., and Liss, P.: Analysis of ammonia and methylamines in natural waters
 680 by flow injection gas diffusion coupled to ion chromatography, *Analytica Chimica Acta*, 316,
 681 291-304, [https://doi.org/10.1016/0003-2670\(95\)00372-7](https://doi.org/10.1016/0003-2670(95)00372-7), 1995.

682 Gibb, S., Mantoura, R., and Liss, P.: Ocean-atmosphere exchange and atmospheric speciation of
 683 ammonia and methylamines in the region of the NW Arabian Sea, *Global Biogeochemical Cycles*



- 684 - GLOBAL BIOGEOCHEM CYCLE, 13, 161-178, <https://doi.org/10.1029/98GB00743>, 1999.
- 685 Gomez-Hernandez, M., McKeown, M., Secrest, J., Marrero-Ortiz, W., Lavi, A., Rudich, Y.,
 686 Collins, D. R., and Zhang, R.: Hygroscopic Characteristics of Alkylammonium Carboxylate Aerosols,
 687 Environmental Science & Technology, 50, 2292-2300, <https://doi.org/10.1021/acs.est.5b04691>,
 688 2016.
- 689 Gorzelska, K., and Galloway, J.: Amine nitrogen in the atmospheric environment over the North
 690 Atlantic Ocean, Global Biogeochemical Cycles - GLOBAL BIOGEOCHEM CYCLE, 4, 309-333,
 691 <https://doi.org/10.1029/GB004i003p00309>, 1990.
- 692 Haque, M., Kawamura, K., Deshmukh, D., Cao, F., Song, W., Bao, M., and Zhang, Y.:
 693 Characterization of organic aerosols from a Chinese megacity during winter: Predominance of
 694 fossil fuel combustion, Atmospheric Chemistry and Physics, 19, 5147-5164,
 695 <https://doi.org/10.5194/acp-19-5147-2019>, 2019.
- 696 He, Q., Ding, X., Fu, X.-X., Zhang, Y.-Q., Wang, J.-Q., Liu, Y.-X., Tang, M.-J., Wang, X., and
 697 Rudich, Y.: Secondary Organic Aerosol Formation from Isoprene Epoxides in the Pearl River
 698 Delta, South China: IEPOX- and HMML-Derived Tracers, Journal of Geophysical Research:
 699 Atmospheres, 123, 6999-7012, <https://doi.org/10.1029/2017JD028242>, 2018.
- 700 Hemmilä, M., Hellén, H., Virkkula, A., Makkonen, U., Praplan, A., Kontkanen, J., Ahonen, L.,
 701 Kulmala, M., and Hakola, H.: Amines in boreal forest air at SMEAR II station in Finland,
 702 Atmospheric Chemistry and Physics, 18, 6367-6380, <https://doi.org/10.5194/acp-18-6367-2018>,
 703 2018.
- 704 Hu, Q., Yu, P., Zhu, Y., Li, K., Gao, H., and Yao, X.: Concentration, Size Distribution, and
 705 Formation of Trimethylammonium and Dimethylammonium Ions in Atmospheric Particles over
 706 Marginal Seas of China*, Journal of the Atmospheric Sciences, 72, 150522112638006,
 707 <https://doi.org/10.1175/JAS-D-14-0393.1>, 2015.
- 708 Huang, S., Song, Q., Hu, W., Yuan, B., Liu, J., Jiang, B., Li, W., Wu, C., Jiang, F., Chen, W., Wang,
 709 X., and Shao, M.: Chemical composition and sources of amines in PM_{2.5} in an urban site of PRD,
 710 China, Environmental Research, 212, 113261, <https://doi.org/10.1016/j.envres.2022.113261>, 2022.
- 711 Johnson, J., and Jen, C.: Role of Methanesulfonic Acid in Sulfuric Acid–Amine and Ammonia
 712 New Particle Formation, ACS Earth and Space Chemistry, 7, 653-660,
 713 <https://doi.org/10.1021/acsearthspacechem.3c00017>, 2023.
- 714 Kang, M., Fu, P., Kawamura, K., Yang, F., Zhang, H., Zang, Z., Ren, H., Ren, L., Zhao, y., Sun, Y.,
 715 and Wang, Z.: Characterization of biogenic primary and secondary organic aerosols in the marine
 716 atmosphere over the East China Sea, Atmospheric Chemistry and Physics, 18, 13947-13967,
 717 <https://doi.org/10.5194/acp-18-13947-2018>, 2018.
- 718 Kleindienst, T., Jaoui, M., Lewandowski, M., Offenberg, J., Lewis, C., Bhawe, P., and Edney, E.:
 719 Estimates of the contributions of biogenic and anthropogenic hydrocarbons to secondary organic
 720 aerosol at a southern US location, Atmospheric Environment, 41, 8288-8300,
 721 <https://doi.org/10.1016/j.atmosenv.2007.06.045>, 2007.



722 Köllner, F., Schneider, J., Willis, M., Klimach, T., Helleis, F., Bozem, H., Kunkel, D., Hoor, P.,
 723 Burkart, J., Leaitch, W. R., Aliabadi, A. A., Abbatt, J., Herber, Andreas B., and Borrmann, S.:
 724 Particulate trimethylamine in the summertime Canadian high Arctic lower troposphere,
 725 Atmospheric Chemistry and Physics, 17, 13747-13766,
 726 <https://doi.org/10.5194/acp-17-13747-2017>, 2017.
 727 Lee, D., and Wexler, A.: Atmospheric amines – Part III: Photochemistry and toxicity, Atmospheric
 728 Environment, 71, 95–103, <https://doi.org/10.1016/j.atmosenv.2013.01.058>, 2013.
 729 Li, G., Liao, Y., Hu, J., Lu, L., Zhang, Y., Li, B., and An, T.: Activation of NF- κ B pathways
 730 mediating the inflammation and pulmonary diseases associated with atmospheric methylamine
 731 exposure, Environmental Pollution, 252, 1216-1224, <https://doi.org/10.1016/j.envpol.2019.06.059>,
 732 2019a.
 733 Li, J., Wang, G., Zhang, q., Li, J., wu, C., Jiang, W., Zhu, T., and Zeng, L.: Molecular
 734 characteristics and diurnal variations of organic aerosols at a rural site in the North China Plain
 735 with implications for the influence of regional biomass burning, Atmospheric Chemistry and
 736 Physics, 19, 10481-10496, <https://doi.org/10.5194/acp-19-10481-2019>, 2019b.
 737 Lidbury, I., Chen, Y., and Murrell, J.: Trimethylamine and trimethylamine N-oxide are
 738 supplementary energy sources for a marine heterotrophic bacterium: Implications for marine
 739 carbon and nitrogen cycling, The ISME Journal, 9, 760-769,
 740 <https://doi.org/10.1038/ismej.2014.149>, 2015.
 741 Lidbury, I., Mausz, M., Scanlan, D., and Chen, Y.: Identification of dimethylamine
 742 monooxygenase in marine bacteria reveals a metabolic bottleneck in the methylated amine
 743 degradation pathway, The ISME Journal, 11, 1592-1601, <https://doi.org/10.1038/ismej.2017.31>,
 744 2017.
 745 Lin, P., Laskin, J., Nizkorodov, S., and Laskin, A.: Revealing Brown Carbon Chromophores
 746 Produced in Reactions of Methylglyoxal with Ammonium Sulfate, Environmental science &
 747 technology, 49, 14257-14266, <https://doi.org/10.1021/acs.est.5b03608>, 2015.
 748 Lin, Q., Zhang, G., Long, P., Bi, X., Wang, X., Brechtel, F., Li, M., Chen, D., Peng, P., amp, apos,
 749 an, Sheng, G., and Zhou, Z.: In situ chemical composition measurement of individual cloud
 750 residue particles at a mountain site, southern China, Atmospheric Chemistry and Physics, 17,
 751 8473-8488, 2017.
 752 Liu, F., Bi, X., Zhang, G., Peng, L., Lian, X., Lu, H., Fu, Y., Wang, X., Peng, P. a., and Sheng, G.:
 753 Concentration, size distribution and dry deposition of amines in atmospheric particles of urban
 754 Guangzhou, China, Atmospheric Environment, 171, 279-288,
 755 <https://doi.org/10.1016/j.atmosenv.2017.10.016>, 2017.
 756 Liu, F., Bi, X., Zhang, G., Lian, X., Fu, Y., Yang, Y., Lin, Q., Jiang, F., Wang, X., Peng, P. a., and
 757 Sheng, G.: Gas-to-particle partitioning of atmospheric amines observed at a mountain site in
 758 southern China, Atmospheric Environment, 195, 1-11,
 759 <https://doi.org/10.1016/j.atmosenv.2018.09.038>, 2018.



760 Liu, T., Xu, Y., Sun, Q., Zhu, R.-G., Li, C. X., Li, Z. Y., Zhang, K. Q., Sun, C. X., and Xiao, H. Y.:
 761 Characteristics, Origins, and Atmospheric Processes of Amines in Fine Aerosol Particles in Winter
 762 in China, *Journal of Geophysical Research: Atmospheres*, 128, e2023JD038974,
 763 <https://doi.org/10.1029/2023JD038974>, 2023.

764 Liu, Z., Li, M., Wang, X., Liang, Y., Jiang, Y., Chen, J., Mu, J., Zhu, Y., Meng, H., Yang, L., Hou,
 765 K., Wang, Y., and Xue, L.: Large contributions of anthropogenic sources to amines in fine particles
 766 at a coastal area in northern China in winter, *Science of The Total Environment*, 839, 156281,
 767 <https://doi.org/10.1016/j.scitotenv.2022.156281>, 2022.

768 Marrero-Ortiz, W., Hu, M., Du, Z., Ji, Y.-M., Wang, Y., Guo, S., Lin, Y., Gomez-Hernandez, M.,
 769 Peng, J., Li, Y., Secrest, J., Levy Zamora, M., Wang, Y., An, T., and Zhang, R.: Formation and
 770 Optical Properties of Brown Carbon from Small α -Dicarbonyls and Amines, *Environmental*
 771 *Science & Technology*, 53, 117-126, <https://doi.org/10.1021/acs.est.8b03995>, 2018.

772 Medeiros, P., Conte, M., Weber, J., and Simoneit, B.: Sugars as source indicators of biogenic
 773 organic carbon in aerosols collected above the Howland Experimental Forest, Maine, *Atmospheric*
 774 *Environment*, 40, 1694-1705, <https://doi.org/10.1016/j.atmosenv.2005.11.001>, 2006.

775 Milne, P., and Zika, R.: Amino acid nitrogen in atmospheric aerosols: Occurrence, sources and
 776 photochemical modification, *Journal of Atmospheric Chemistry*, 16, 361-398,
 777 <https://doi.org/10.1007/BF01032631>, 1993.

778 Miyazaki, Y., Kawamura, K., and Sawano, M.: Size distributions and chemical characterization of
 779 water-soluble organic aerosols over the western North Pacific in summer, *J. Geophys. Res.*, 115,
 780 <https://doi.org/10.1029/2010JD014439>, 2010.

781 Mochida, M., Kawabata, A., Kawamura, K., Hatsushika, H., and Yamazaki, K.: Seasonal variation
 782 and origin of dicarboxylic acids in the marine atmosphere over the western North Pacific, *Journal*
 783 *of Geophysical Research*, 108, <https://doi.org/10.1029/2002JD002355>, 2003.

784 Müller, C., Iinuma, Y., Karstensen, J., Pinxteren, D., S, L., T, G., and Herrmann, H.: Seasonal
 785 variation of aliphatic amines in marine sub-micrometer particles at the Cape Verde Islands,
 786 *Atmospheric Chemistry and Physics*, 9, 9587-9597, <https://doi.org/10.5194/acpd-9-14825-2009>,
 787 2009.

788 Murphy, S., Sorooshian, A., Kroll, J., Ng, N., Chhabra, P., C, T., Surratt, J., Knipping, E., Flagan,
 789 R., and Seinfeld, J.: Secondary aerosol formation from atmospheric reactions of aliphatic amines,
 790 *Atmospheric Chemistry and Physics Discussions*, 7, 289-349,
 791 <https://doi.org/10.5194/acp-7-2313-2007>, 2007.

792 Myriokefalitakis, S., Elisabetta, V., Tsigaridis, K., Papadimas, C. D., Sciare, J., Mihalopoulos, N.,
 793 Facchini, M., Matteo, R., Dentener, F., Ceburnis, D., Hatzianastassiou, N., O'Dowd, C., van Weele,
 794 M., and Kanakidou, M.: Global Modeling of the Oceanic Source of Organic Aerosols, *Advances*
 795 *in Meteorology*, 2010, 2010, <https://doi.org/10.1155/2010/939171>, 2010.

796 Nakamura, T., Matsumoto, K., and Uematsu, M.: Chemical characteristics of aerosols transported
 797 from Asia to the East China Sea: An evaluation of anthropogenic combined nitrogen deposition in



798 autumn, Atmospheric Environment, 39, 1749-1758,
 799 <https://doi.org/10.1016/j.atmosenv.2004.11.037>, 2005.

800 Namieśnik, J., Jastrzebska, A., and Zygmunt, B.: Determination of volatile aliphatic amines in air
 801 by solid-phase microextraction coupled with gas chromatography with flame ionization detection,
 802 Journal of chromatography. A, 1016, 1-9, [https://doi.org/10.1016/S0021-9673\(03\)01296-2](https://doi.org/10.1016/S0021-9673(03)01296-2), 2003.

803 Ng, N., Jimenez, J., Chhabra, P., Seinfeld, J., and Worsnop, D.: Changes in organic aerosol
 804 composition with aging inferred from aerosol mass spectra, Atmospheric Chemistry and Physics -
 805 ATMOS CHEM PHYS, 11, 6465-6474, <https://doi.org/10.5194/acp-11-6465-2011>, 2011.

806 Nielsen, C. J., Herrmann, H., and Weller, C.: Atmospheric chemistry and environmental impact of
 807 the use of amines in carbon capture and storage (CCS), Chem Soc Rev, 41, 6684-6704,
 808 <https://doi.org/10.1039/c2cs35059a>, 2012.

809 Pankow, J.: Phase Considerations in the Gas/Particle Partitioning of Organic Amines in the
 810 Atmosphere, Atmospheric Environment, 122, 448-453,
 811 <https://doi.org/10.1016/j.atmosenv.2015.09.056>, 2015.

812 Pinxteren, M. V., Fomba, K., Pinxteren, D., Triesch, N., Hoffmann, E., Cree, C., Fitzsimons, M.,
 813 Tümpling, W., and Herrmann, H.: Aliphatic amines at the Cape Verde Atmospheric Observatory:
 814 Abundance, origins and sea-air fluxes, Atmospheric Environment, 203, 183-195,
 815 <https://doi.org/10.1016/j.atmosenv.2019.02.011>, 2019.

816 Place, B., Quilty, A., Lorenzo, R., Ziegler, S., and VandenBoer, T.: Quantitation of 11 alkyl amines
 817 in atmospheric samples: Separating structural isomers by ion chromatography, Atmospheric
 818 Measurement Techniques, 10, 1061-1078, <https://doi.org/10.5194/amt-10-1061-2017>, 2017.

819 Price, D., Clark, C., Tang, X., Cocker, D., Purvis-Roberts, K., and Silva, P.: Proposed chemical
 820 mechanisms leading to secondary organic aerosol in the reactions of aliphatic amines with
 821 hydroxyl and nitrate radicals, Atmospheric Environment, 96, 135-144,
 822 <https://doi.org/10.1016/j.atmosenv.2014.07.035>, 2014.

823 Price, D., Kacarab, M., Cocker, D., Purvis-Roberts, K., and Silva, P.: Effects of Temperature on
 824 the Formation of Secondary Organic Aerosol from Amine Precursors, Aerosol Science and
 825 Technology, 50, 1216-1226, <https://doi.org/10.1080/02786826.2016.1236182>, 2016.

826 Qiu, C., and Zhang, R.: Multiphase chemistry of atmospheric amines, Physical chemistry chemical
 827 physics, 15, 5738-5752, <https://doi.org/10.1039/c3cp43446j>, 2013.

828 Rinaldi, M., Decesari, S., Finessi, E., Giulianelli, L., Carbone, C., Fuzzi, S., O'Dowd, C. D.,
 829 Ceburnis, D., and Facchini, M. C.: Primary and Secondary Organic Marine Aerosol and Oceanic
 830 Biological Activity: Recent Results and New Perspectives for Future Studies, Advances in
 831 Meteorology, 2010, 1-10, <https://doi.org/10.1155/2010/310682>, 2010.

832 Rogge, W., Hildemann, L., Mazurek, M., Cass, G., and Simoneit, B.: Sources of Fine Organic
 833 Aerosol. 3. Road Dust, Tire Debris, and Organometallic Brake Lining Dust: Roads as Sources and
 834 Sinks, Environmental Science & Technology - ENVIRON SCI TECHNOL, 27, 1892-1904,
 835 <https://doi.org/10.1021/es00046a019>, 1993.



836 Schade, G., and Crutzen, P.: Emission of aliphatic amines from animal husbandry and their
 837 reactions: Potential source of N₂O and HCN, *Journal of Atmospheric Chemistry*, 22, 319-346,
 838 <https://doi.org/10.1007/BF00696641>, 1995.

839 Shen, J., Xie, H.-B., Elm, J., ma, F., Chen, J., and Vehkamäki, H.: Methanesulfonic Acid-driven
 840 New Particle Formation Enhanced by Monoethanolamine: A Computational Study, *Environmental*
 841 *Science & Technology*, <https://doi.org/10.1021/acs.est.9b05306>, 2019.

842 Shen, W., Ren, L., Zhao, Y., Zhou, L., Dai, L., Ge, X., Kong, S., Yan, Q., Xu, H., Jiang, Y., He, J.,
 843 Chen, M., and Yu, H.: C1-C2 alkyl aminiums in urban aerosols: Insights from ambient and fuel
 844 combustion emission measurements in the Yangtze River Delta region of China, *Environ Pollut*,
 845 230, 12-21, <https://doi.org/10.1016/j.envpol.2017.06.034>, 2017.

846 Shen, X., Chen, J., and An, T.: A new advance in pollution profile, transformation process, and
 847 contribution to SOA formation of atmospheric organic amines, *Environmental Science:*
 848 *Atmospheres*, 3, 444-473, <https://doi.org/10.1039/D2EA00167E>, 2023.

849 Simoneit, B., Sheng, G., Chen, X., Fu, J., Zhang, J., and Xu, Y.: Molecular marker study of
 850 extractable organic matter in aerosols from urban areas of China, *Atmospheric Environment. Part*
 851 *A. General Topics*, 25, 2111-2129, [https://doi.org/10.1016/0960-1686\(91\)90088-O](https://doi.org/10.1016/0960-1686(91)90088-O), 1991.

852 Simoneit, B., Elias, V., Kobayashi, M., Kawamura, K., Rushdi, A., Medeiros, P., Rogge, W., and
 853 Didyk, B.: SugarsDominant Water-Soluble Organic Compounds in Soils and Characterization as
 854 Tracers in Atmospheric Particulate Matter, *Environmental science & technology*, 38, 5939-5949,
 855 <https://doi.org/10.1021/es0403099>, 2004.

856 Sorooshian, A., Murphy, S., Hersey, S., H, G., Padro, L., Nenes, A., Brechtel, F., Jonsson, H.,
 857 Flagan, R., and Seinfeld, J.: Comprehensive airborne characterization of aerosol from a major
 858 bovine source, *Atmospheric Chemistry and Physics Discussions*, 8, 10415-10479,
 859 <https://doi.org/10.5194/acp-8-5489-2008>, 2008.

860 Sorooshian, A., Padro, L., Nenes, A., Feingold, G., McComiskey, A., Hersey, S., Gates, H.,
 861 Jonsson, H., Miller, S., and Stephens, G.: On the Link Between Ocean Biota Emissions, Aerosol,
 862 and Maritime Clouds: Airborne, Ground, and Satellite Measurements Off the Coast of California,
 863 *Global Biogeochem. Cycles*, 23, 34, <https://doi.org/10.1029/2009GB003464>, 2009.

864 Sun, J., Mausz, M., Chen, Y., and Giovannoni, S.: Microbial Trimethylamine Metabolism in
 865 Marine Environments: Microbial TMA metabolism, *Environmental Microbiology*, 21, 513-520,
 866 <https://doi.org/10.1111/1462-2920.14461>, 2019.

867 Tang, X., Price, D., Praske, E., Lee, S. A., Shattuck, M. A., Purvis-Roberts, K., Silva, P. J.,
 868 Asa-Awuku, A., and Cocker, D. R.: NO₃ radical, OH radical and O₃-initiated secondary aerosol
 869 formation from aliphatic amines, *Atmospheric Environment*, 72, 105-112,
 870 <https://doi.org/10.1016/j.atmosenv.2013.02.024>, 2013.

871 Tang, X., Price, D., Praske, E., Vu, D. N., Purvis-Roberts, K., Silva, P. J., Cocker Iii, D. R., and
 872 Asa-Awuku, A.: Cloud condensation nuclei (CCN) activity of aliphatic amine secondary aerosol,
 873 *Atmospheric Chemistry and Physics*, 14, 5959-5967, <https://doi.org/10.5194/acp-14-5959-2014>,



- 2014.
- Van Neste, A., Duce, R. A., and Lee, C.: Methylamines in the Marine Atmosphere, *Geophysical Research Letters - GEOPHYS RES LETT*, 14, 711–714, <https://doi.org/10.1029/GL014i007p00711>, 1987.
- VandenBoer, T., Markovic, M., Petroff, A., Czar, M. F., Borduas, N., and Murphy, J. G.: Ion chromatographic separation and quantitation of alkyl methylamines and ethylamines in atmospheric gas and particulate matter using preconcentration and suppressed conductivity detection, *Journal of chromatography. A*, 1252, 74-83, <https://doi.org/10.1016/j.chroma.2012.06.062>, 2012.
- Violaki, K., and Mihalopoulos, N.: Water-soluble organic nitrogen (WSON) in size-segregated atmospheric particles over the Eastern Mediterranean, *Atmospheric Environment*, 44, 4339-4345, <https://doi.org/10.1016/j.atmosenv.2010.07.056>, 2010.
- Wang, X.-C., and Lee, C.: Sources and distribution of aliphatic amines in salt marsh sediment, *Organic Geochemistry - ORG GEOCHEM*, 22, 1005-1021, [https://doi.org/10.1016/0146-6380\(94\)90034-5](https://doi.org/10.1016/0146-6380(94)90034-5), 1994.
- Welsh, D.: Ecological significance of compatible solute accumulation by micro- organisms: From single cells to global climate, *FEMS Microbiology Reviews*, 24, 263-290, <https://doi.org/10.1111/j.1574-6976.2000.tb00542.x>, 2000.
- Xie, H., Feng, L., Hu, Q., Zhu, Y., Gao, H., Gao, Y., and Yao, X.: Concentration and size distribution of water-extracted dimethylaminium and trimethylaminium in atmospheric particles during nine campaigns - Implications for sources, phase states and formation pathways, *The Science of the total environment*, 631-632, 130-141, <https://doi.org/10.1016/j.scitotenv.2018.02.303>, 2018.
- Yang, H., Xu, J., Wu, W.-S., Wan, C., and Yu, J.: Chemical Characterization of Water-Soluble Organic Aerosols at Jeju Island Collected During ACE-Asia, *Environmental Chemistry - ENVIRON CHEM*, 1, 13-17, <https://doi.org/10.1071/EN04006>, 2004.
- Yang, X.-Y., Cao, F., Fan, M., Lin, Y. C., Xie, F., and Zhang, Y.: Seasonal variations of low molecular alkyl amines in PM_{2.5} in a North China Plain industrial city: Importance of secondary formation and combustion emissions, *The Science of the total environment*, 857, 159371, <https://doi.org/10.1016/j.scitotenv.2022.159371>, 2023.
- Yao, L., Garmash, O., Bianchi, F., Zheng, J., Yan, C., Kontkanen, J., Junninen, H., Mazon, S., Ehn, M., Paasonen, P., Sipilä, M., Wang, M., Wang, X., Xiao, S., Chen, H., Lu, Y., Zhang, B., Wang, D., Fu, Q., and Wang, L.: Atmospheric new particle formation from sulfuric acid and amines in a Chinese megacity, *Science*, 361, 278-281, <https://doi.org/10.1126/science.aao4839>, 2018.
- Yin, S., Ge, M.-F., Wang, W., Liu, Z., and Wang, D.: Uptake of gas-phase alkylamines by sulfuric acid, *Chinese Science Bulletin*, 56, 1241-1245, <https://doi.org/10.1007/s11434-010-4331-9>, 2011.
- You, Kanawade, V., de Gouw, J., Guenther, A., Madronich, S., Sierra-Hernández, M., Lawler, M., Smith, J., Takahama, S., Ruggeri, G., Koss, A., Olson, K., Baumann, K., Weber, R., Nenes, A.,



912 Guo, H., Edgerton, E., Porcelli, L., Brune, W., and Lee, S.-H.: Atmospheric amines and ammonia
 913 measured with a Chemical Ionization Mass Spectrometer (CIMS), *Atmospheric Chemistry and*
 914 *Physics*, 14, 12181-12194, <https://doi.org/10.5194/acp-14-12181-2014>, 2014.

915 Yu, P., Hu, Q., Li, K., Zhu, Y., Liu, X., Gao, H., and Yao, X.: Characteristics of dimethylammonium
 916 and trimethylammonium in atmospheric particles ranging from supermicron to nanometer sizes over
 917 eutrophic marginal seas of China and oligotrophic open oceans, *Science of The Total Environment*,
 918 572, 813-824, <https://doi.org/10.1016/j.scitotenv.2016.07.114>, 2016.

919 Zhang, H., Surratt, J., Lin, Y.-H., Bapat, J., and Kamens, R.: Effect of relative humidity on SOA
 920 formation from isoprene/NO photooxidation: Enhancement of 2-methylglyceric acid and its
 921 corresponding oligoesters under dry conditions, *Atmospheric Chemistry and Physics - ATMOS*
 922 *CHEM PHYS*, 11, 6411-6424, <https://doi.org/10.5194/acp-11-6411-2011>, 2011.

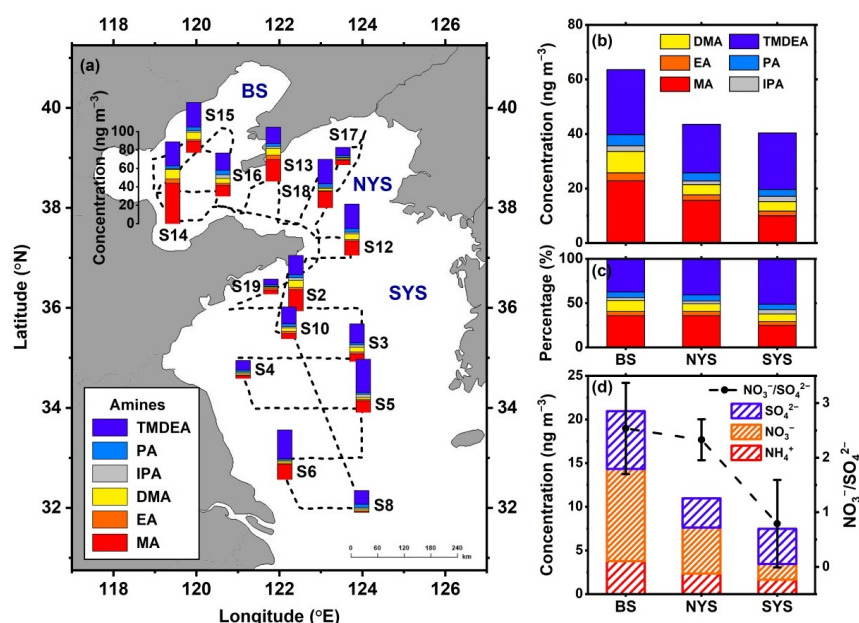
923 Zheng, J., Ma, Y., Chen, M., Zhang, Q., Wang, L., Khalizov, A. F., Yao, L., Wang, Z., Wang, X.,
 924 and Chen, L.: Measurement of atmospheric amines and ammonia using the high resolution
 925 time-of-flight chemical ionization mass spectrometry, *Atmospheric Environment*, 102, 249-259,
 926 <https://doi.org/10.1016/j.atmosenv.2014.12.002>, 2015.

927 Zheng, L., Yang, X., Lai, S., Ren, H., Yue, S., Zhang, Y., Huang, X., Gao, Y., Sun, Y., Wang, Z.,
 928 and Fu, P.: Impacts of springtime biomass burning in the northern Southeast Asia on marine
 929 organic aerosols over the Gulf of Tonkin, China, *Environmental pollution (Barking, Essex : 1987)*,
 930 237, 285-297, <https://doi.org/10.1016/j.envpol.2018.01.089>, 2018.

931 Zhou, S., Li, H., Yang, T., Chen, Y., Deng, C., Gao, Y., Chen, C., and Xu, J.: Characteristics and
 932 sources of aerosol aminiums over the eastern coast of China: insights from the integrated
 933 observations in a coastal city, adjacent island and surrounding marginal seas, *Atmospheric*
 934 *Chemistry and Physics*, 19, 10447-10467, <https://doi.org/10.5194/acp-19-10447-2019>, 2019.

935 Zhu, S., Yan, C., Zheng, J., Chen, C., Ning, H., Yang, D., Wang, M., Ma, Y., Zhan, J., Hua, C., Yin,
 936 R., Li, Y., Liu, Y., Jiang, J., Yao, L., Wang, L., Kulmala, M., and Worsnop, D.: Observation and
 937 Source Apportionment of Atmospheric Alkaline Gases in Urban Beijing, *Environmental Science*
 938 *& Technology*, 56, 17545-17555, <https://doi.org/10.1021/acs.est.2c03584>, 2022.

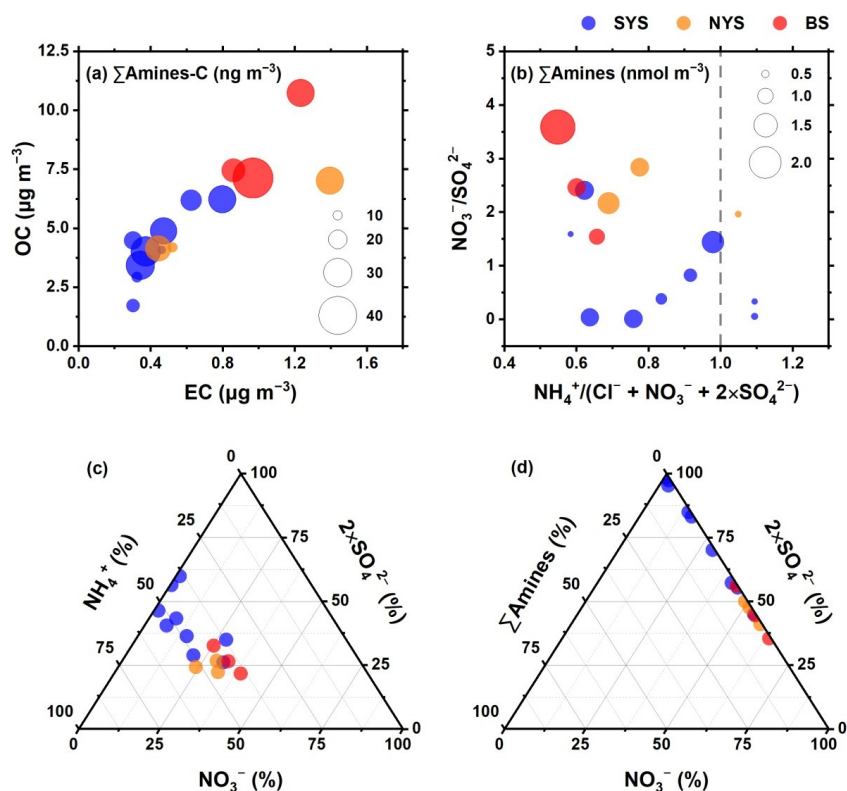
939



940

941 **Figure 1.** Concentrations of amines in 15 TSP samples (a) collected along the cruise
 942 track (black dotted line); average concentrations (b) and relative contributions (c) of
 943 amines; and concentrations of NH_4^+ , NO_3^- , and SO_4^{2-} , along with $\text{NO}_3^-/\text{SO}_4^{2-}$ molar
 944 ratios (d), in TSP over the SYS, NYS, and BS.

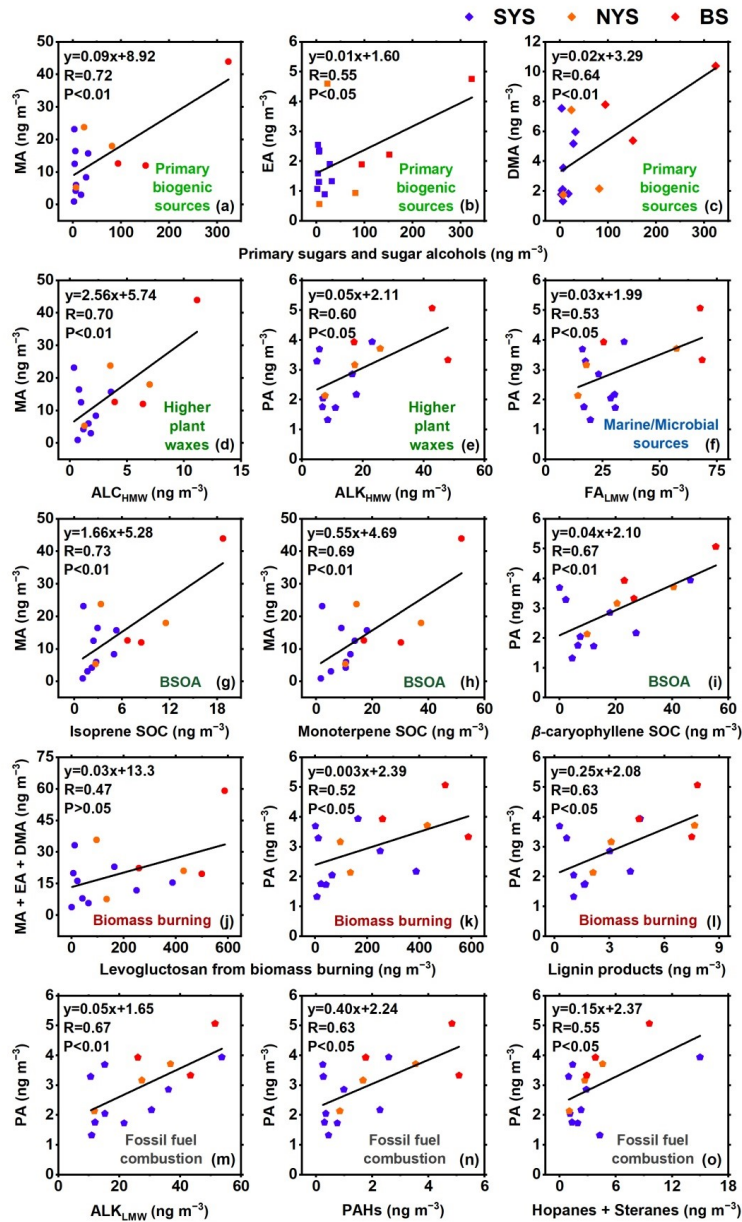
945



946

947 **Figure 2.** Variations of $\Sigma \text{amines-C}$ with OC and EC concentrations (a); variations of
 948 Σamines molar concentrations with the $\text{NO}_3^-/\text{SO}_4^{2-}$ and $\text{NH}_4^+/(\text{Cl}^- + \text{NO}_3^- + 2 \times \text{SO}_4^{2-})$
 949 molar ratios (b); ternary diagram of the molar ratio of NH_4^+ , NO_3^- , and SO_4^{2-} (c); and
 950 ternary diagram of the molar ratio of Σamines , NO_3^- , and SO_4^{2-} (d) in TSP over the
 951 SYS, NYS, and BS.

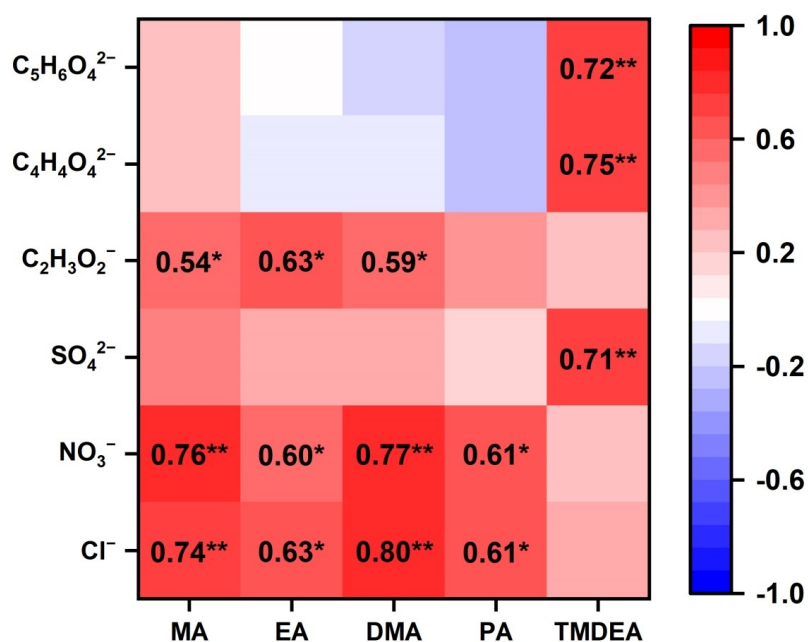
952



953

954 **Figure 3.** Linear regressions between amines and biomarkers (a–i), biomass burning
955 tracers (j–l), and fossil fuel combustion tracers (m–o) in TSP over the SYS, NYS, and
956 BS.

957



958

959 **Figure 4.** Correlation coefficient matrix between amines and acidic species in TSP
 960 over the YS–BS. Numbers indicate correlation coefficients that passed the
 961 significance test; ** denotes $P < 0.01$, and * denotes $P < 0.05$.

962

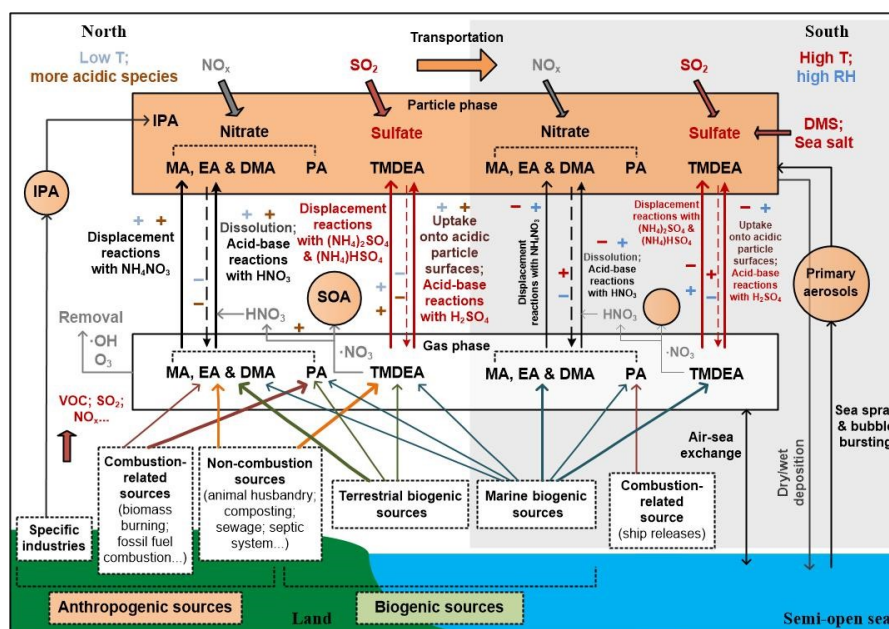


Figure 5. Schematic diagram illustrating the source contributions and major secondary formation mechanisms of amines, along with the influences of environmental conditions over the YS–BS.